Appl Nanosci (2013) 3:383–388
DOI 10.1007/s13204-012-0146-0

ORIGINAL ARTICLE

Absence of free carrier and paramagnetism in cobalt-doped ZnO nanoparticles synthesized at low temperature using citrate sol–gel route

A. Sivagamasundari · R. Pugaze · S. Chandrasekar · S. Rajagopan · R. Kannan

Received: 20 April 2012 / Accepted: 28 June 2012 / Published online: 24 July 2012

Abstract Cobalt-doped ZnO nanoparticles have been synthesized using a simple citrate sol–gel auto-combustion method. The XRD confirms nano-single phase and Wurtzite structure. Increased cobalt solubility from 15 to 20 % was observed in ZnO matrix due to low temperature synthesis. Room temperature paramagnetic contribution is observed for all the samples, since cobalt is a neutral dopant and no free carriers are produced. Normally, ferromagnetism is observed in ZnO due to carrier mediated interaction between transition metal ions and free carriers. Hence no ferromagnetism was observed and only paramagnetism was observed due to non-availability of free carriers for long range ferromagnetic interaction in our system. At higher doping, peak broadening of the highly intense XRD peak (101) was observed indicating formation of cobalt cluster (metal–metal) which reduces paramagnetism due to antiferromagnetic interaction and the magnetization value decreases to 0.00456 from 0.0076 emu/g. Absence of photoluminescence peak at 520 nm due to oxygen related defects also supports, the presence of paramagnetism in our samples, since oxygen defects are the another source of ferromagnetism in ZnO. Indirect evidence for the presence of cobalt clustering is also obtained from the photoluminescence studies which lead to concentration quenching of peaks. Photoluminescence studies exhibit NBE peak at 412 nm and defect peaks at 471 and 672 nm. The intensity of red emission peak at 672 nm remains constant whereas the intensity of the peaks at 412 and 471 nm increases and then decreases due to doping induced disorder leading to concentration quenching.

Keywords Citrate sol–gel low temperature synthesis · Solubility · Absence of free carriers · Paramagnetic study · Photoluminescence

A. Sivagamasundari · R. Pugaze · S. Chandrasekar · R. Kannan (✉)
Department of Physics, Pondicherry Engineering College, Puducherry 605 014, India
e-mail: kannan@pec.edu

A. Sivagamasundari
e-mail: sivaakaash@gmail.com

S. Rajagopan
Department of Chemistry, Pondicherry Engineering College, Puducherry 605 014, India

Introduction

ZnO is a wide band gap (3.37 eV) semiconductor with a large exciton binding energy (60 meV) possessing unique photonic and spintronic properties (Segawa et al. 1997). 3d transition metal (Co, Ni, Mn, Cu, Cr, V and Fe)-doped wide band gap oxides, such as ZnO, TiO_2 and SnO_2, are preferred for their high T_c, compared to traditional III–V series such as GaN, GaAs, InP and GaP, for room temperature ferromagnetism applications (Dietl et al. 2000; Hammad and Salem 2011). ZnO exhibits visible luminescence even though excitation is carried out at different UV wavelengths due to formation of different types of defects. Transition metal doping of ZnO enhances optical absorption leading to changes in the band gap which makes the semiconductor to be more effective photo catalyst, leading to the development of novel magneto-optoelectronic devices (Lebedeva and Kuivalainen 2003; Ando et al. 2001a, b).

Room temperature ferromagnetism in ZnO is not yet resolved even though a large number of theories were proposed. Room temperature ferromagnetism in ZnO is

connected to free carriers and production of free carriers either by doping (p or n type) or by some other method is a necessary condition for room temperature ferromagnetism. Lot of contradictory reports are available on transition metal-doped ZnO, giving rise to ferromagnetism or paramagnetism depending upon the preparation conditions. The site occupancy of dopant atom (lattice or interstitial) is important and whether it produces free carriers in the form of shallow acceptor or donor levels, to decide the nature of magnetism in ZnO.

Carrier-mediated ferromagnetism is designed to explain room temperature ferromagnetism in DMS following Zener (1950) model and formation of defect with free carriers leading to bound magnetic polaron (BMP) is proposed by Coey et al. (2005) to explain room temperature ferromagnetism in transition metal-doped systems. After the discovery of ferromagnetism in all (conducting, semiconducting and insulating) nano-oxide materials (Sundaresan et al. 2006), such as CeO_2, HfO_2, Al_2O_3, SnO_2, In_2O_3, ZnO, etc., oxygen-related defect-induced ferromagnetism is sought to explain the observed room temperature ferromagnetism. Recently non-magnetic materials such as aluminum, gallium and nitrogen doped in ZnO produced room temperature ferromagnetism giving rise to carrier induced ferromagnetism. Hence it is understood that free carriers are the essential requirement for room temperature ferromagnetism whatever may be the mechanism proposed for room temperature ferromagnetism in ZnO.

Several groups observed the ferromagnetism in $Zn_{1-x}Co_xO$ nanoparticles by a variety of preparation methods, such as hydrothermal technique, pulsed laser deposition, ball-milling and sol–gel etc (Yang et al. 2006; Wang et al. 2012; Sarsari et al. 2011). Lee et al. (2002) also reported ferromagnetism above 350 K in cobalt-doped ZnO films synthesized by the sol–gel method having solubility up to 20 % and beyond 25 % impurity peak was found and the observed ferromagnetism is attributed to increased free carrier concentration. Ueda et al. (2001) reported ferromagnetism with a Curie temperature higher than room temperature for the cobalt-doped ZnO films grown by the pulsed laser deposition technique. The origin of room temperature ferromagnetism in cobalt-doped ZnO still remains controversial.

Some research groups reported no ferromagnetism in their nanocrystalline powders of cobalt-doped ZnO samples (Risbud et al. 2003; Bouloudenine et al. 2004; Rao and Deepak 2005). Risbud et al. (2003) prepared nanopowders of $Zn_{1-x}Co_xO$ ($x = 0.05$–0.30) with (particle sizes in the 50–200 nm) using zinc and cobalt oxalates synthesized at a temperature of 1,173 K and the magnetism is attributed to the interaction between isolated cobalt ions and paired cobalt ions giving rise to paramagnetic and antiferromagnetic interactions coexist. Zhang et al. (2006a, b) also confirmed the same from Rutherford backscattering channeling technique (RBS) studies. Bouloudenine et al. (2004) reported that no distinct ferromagnetic behavior due to the absence of free carriers was observed in $Zn_{1-x}Co_xO$ ($x = 0.10$) with particle size of around 100 nm, prepared by hydrothermal technique at 240 °C (Rao and Deepak 2005) observed the absence of ferromagnetism in cobalt-doped ZnO powders with particle sizes of 30–50 nm prepared by low temperature decomposition of acetate solid solutions and absence of ferromagnetism is attributed to absence of free carriers in the system.

In the present work, we have prepared cobalt-doped ZnO at a temperature of 450 °C without any secondary phases using sol–gel auto-combustion technique and paramagnetism was observed as a result of no free carriers are available, as cobalt in the ZnO lattice goes as neutral impurity in the lattice without giving rise to free carriers but acts as isolated transition metal ion with local 3d spin.

Experimental procedure

Cobalt-doped ZnO nanoparticles were synthesized by sol–gel method using citric acid as a precursor. Zinc nitrate hexahydrate (99.9 %), cobalt nitrate hexahydrate (99 %), citric acid (99 %), 30 % ammonia solution are used as reactants. All aqueous metal nitrates were added to citric acid under constant stirring. Metal complexing is observed after addition of 30 % ammonia solution until pH is 9.0 and pink color change was observed. The gel was evaporated and combustion was observed at 100 °C and the resultant powder was calcined at 450 °C for 8 h.

The structural properties of $Zn_{1-x}Co_xO$ powders were studied by XRD (Xpert PROPANalytic X-ray diffractometer at Karaikudi Alagappa university) using monochromatic Cu-K_α radiation for 2θ values from 10^o to 80^o at room temperature. Magnetic and photoluminescence studies were carried out using VSM (Vibrating sample magnetometer of range 1.4 T, SAIF, IIT Madras) and Spectroflurometer (Flourolog-3range form 180–1550 nm, CIF, Pondicherry University).

Results and discussion

Powder X-ray diffraction (XRD) pattern of the samples of $Zn_{1-x}Co_xO$ ($x = 0.05, 0.1, 0.15, 0.2$ and 0.25) are shown in Fig. 1. The diffraction patterns of the samples confirm wurtzite structure of ZnO. No other peaks corresponding to cobalt related secondary or impurity phase was found in cobalt-doped ZnO sample, which may be attributed to the incorporation of cobalt ion into the Zn lattice site.

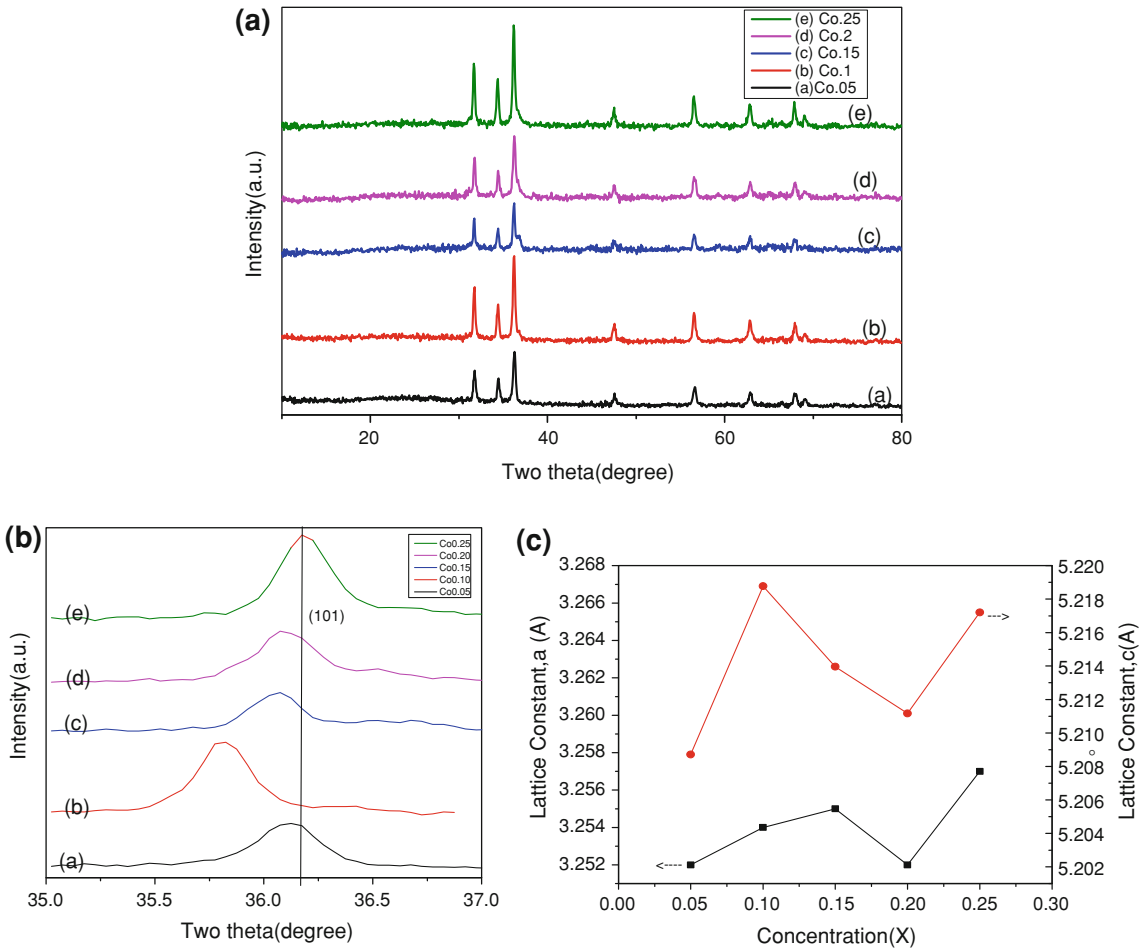

Fig. 1 **a** Powder XRD patterns of $Zn_{1-x}Co_xO$. **b** Shifting of (101) XRD peak as a function of concentration. **c** Variation of the lattice parameters versus Co concentration

The average grain size (D) of the crystallite was estimated from the FWHM of XRD lines by using the Debye–Scherrer formula

$$D = K\lambda/\beta\cos\theta,$$

where, K is the particle shape factor (0.9), λ is the wavelength of Cu-K_α radiation (1.5406), β is the full width at half maximum (FWHM) of the XRD peak and θ is the diffraction angle of the peak.

It can be seen that the average size of nanoparticles decreased from 25 to 14 nm as the doping concentration of cobalt metal is increased from $x = 0.05$ to 0.20, which is attributed to the variance in the ionic radii of cobalt (0.58 Å) and zinc (0.60 Å) (Shannon and Prewitt 1969; Shannon 1976) as shown in Table 1. Shifting of the XRD 101 peak was found as a function of doping concentration, which is attributed to size reduction and consequent lattice strain is responsible for the peak shift (Pal and Giri 2010). With increasing x, the particle size gradually decreases and shows rapid changes for $x > 0.20$, indicating that cobalt incorporation into the ZnO lattice decreases the particle size (Hays et al. 2005, 2007).

As a function of doping concentration, when x increases particle size decreases gradually from 25 nm for $x = 0.05$ to 14 nm for $x = 0.20$ indicating cobalt substitution in the ZnO lattice decreases the grain size from 25 to 14 nm. For cobalt concentration of ($x = 0.25$) the particle size suddenly increases from 14 to 29 nm and the change in the particle size is responsible for strain induced in the lattice. Consequently strain is responsible for cobalt clustering. Most of the existing reports explain that cobalt has a limited solubility in ZnO up to ~15 % (Zhang et al. 2006a, b; Rath et al. 2009; Bhat and Deepak 2005; Seunghun Lee et al. 2012). In our case the doped solubility limit is increased to 20 % which is attributed to nanophasic nature of ZnO synthesized via sol–gel method at low temperature. Moreover, Risbud et al. (2003) have also found that cobalt solubility in ZnO is beyond 20 % when oxalate precursors are sintered at 1,173 K.

Figure 2a and b shows the magnetic properties of cobalt-doped ZnO nanoparticles investigated using

Table 1 The lattice parameters and crystallite size of Zn_{1-x} Co_xO system

Sample	a (Å)	c (Å)	c/a ratio	D_{ave} (nm)
$Zn_{0.95}$ $Co_{0.05}O$	3.25219	5.20411	1.600	25.0557
$Zn_{0.90}Co_{0.10}O$	3.25468	5.21311	1.601	23.7990
$Zn_{0.85}Co_{0.15}O$	3.25595	5.20886	1.600	19.5323
$Zn_{0.80}Co_{0.20}O$	3.25272	5.20634	1.600	14.9493
$Zn_{0.75}Co_{0.25}O$	3.25774	5.21174	1.600	29.9615

Table 2 The magnetic saturation and particle size values of Zn_{1-x} Co_xO

Sample	Saturation magnetization in emu/g	Particle size (nm)
$Zn_{0.95}$ $Co_{0.05}O$	0.00372	25.0557
$Zn_{0.90}Co_{0.10}O$	0.00753	23.7990
$Zn_{0.85}Co_{0.15}O$	0.00645	19.5323
$Zn_{0.80}Co_{0.20}O$	0.00682	14.9493
$Zn_{0.75}Co_{0.25}O$	0.00456	29.9615

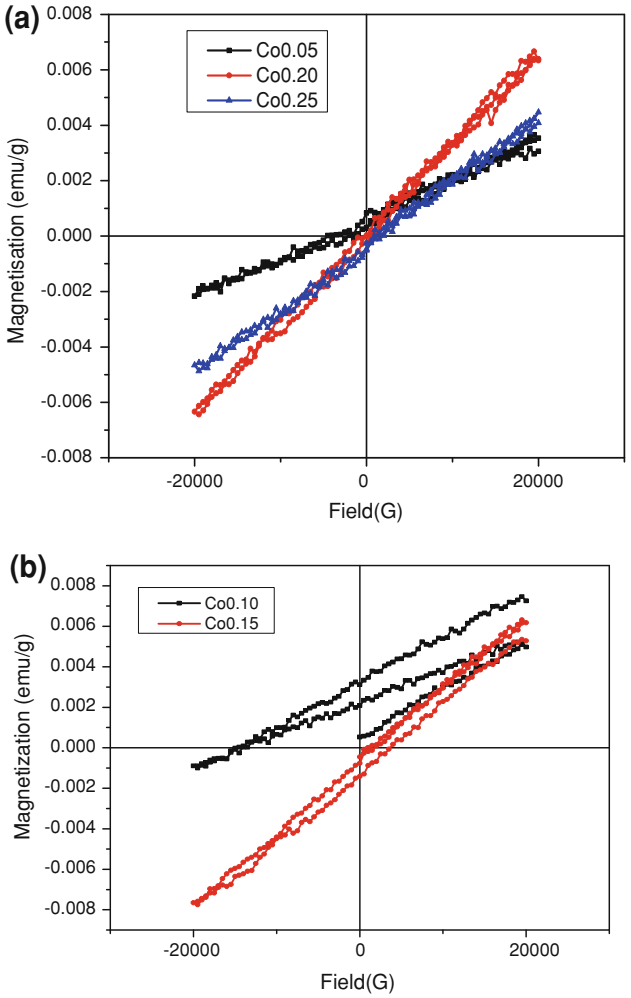

Fig. 2 **a** M–H curves of Zn_{1-x} Co_xO (0.05, 0.20 and 0.25) at room temperature. **b** M–H curves of Zn_{1-x} Co_xO (0.10 and 0.15) at room temperature

vibrating sample magnetometer as shown in Table 2. For non-saturating field, when cobalt ion ($x = 0.05$ and 0.10) is doped in ZnO, it exhibits large paramagnetic behavior. In ZnO, ferromagnetism arises due to carrier mediated interaction between transition metal ions and free carriers. Shi et al. (2010) reported that cobalt is a neutral dopant atom which do not produce free carriers from X-ray absorption near-edge structure (XANES) studies. Hence, non availability of free carriers is responsible for the observed paramagnetism in our sample.

Moreover according to mean-field theory (Jayanthi et al. 2010) observed ferromagnetism in $Zn_{1-x}TM_xO$, which is attributed to interaction between transition metal atoms and free carriers giving rise to ferromagnetism. It is evident as free carriers are not available, paramagnetism was observed in our system. Moreover, in support of our argument Bouloudenine et al. (2004) reported that the observed paramagnetism is due to absence of free carriers. Also the other source of ferromagnetism in ZnO is due to the presence of oxygen related defects. Pal and Giri (2010) assigned the presence of 520 nm peak in photoluminescence to oxygen related defects. The absence of 520 nm peak in our photoluminescence spectra may be attributed to absence of ferromagnetism as no oxygen related defects are present in the sample.

In Fig. 2b, magnetization-field curves of the compound $Zn_{0.90}Co_{0.10}O$ and $Zn_{0.85}Co_{0.15}O$ appear to be different because of coexistence of paramagnetism as well as antiferromagnetism. The differences in the coordination of cobalt atom (changes in the nearest neighbors due to clustering) giving rise to small change in coordination tetrahedra, neighboring defects and local lattice distortions may lead to different magnetic behavior, is responsible for the displacement of magnetization curve (Kobayashi et al. 2005).

Further increasing cobalt concentration ($x = 0.15$, 0.20 and 0.25) no impurity peak was found. But the broadening of (101) peak was found indicating cobalt is segregated at grain boundary which further reduces the paramagnetism due to Co–Co metal cluster antiferromagnetic interactions (Garcia et al. 2010; Quesada et al. 2006). Already reports are available that high cobalt concentration would produce poor crystallization leading to a disturbance in regular arrangement of the magnetic moment (Ma et al. 2008). As a result, magnetization values are reduced due to low magnetic moment order. In favor of this Pal and Giri (2010) reported the absence of ferromagnetism and transition to paramagnetism is attributed to possible

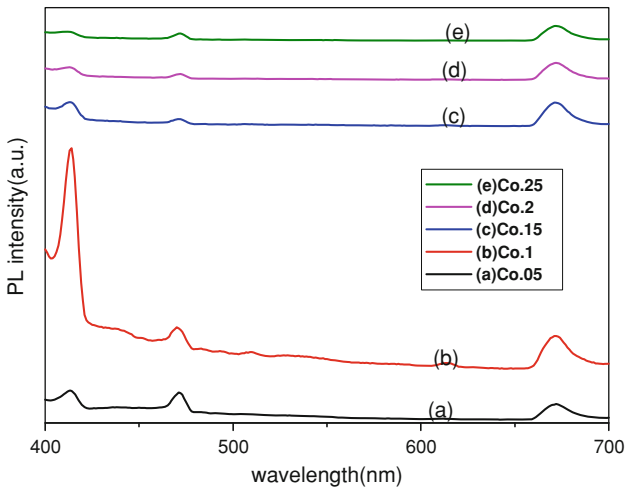

Fig. 3 Photoluminescence spectra of Zn_{1-x} Co_xO

antiferromagnetic interactions due to the reduction in average interatomic distance of doped cobalt ions which is supported by the changes in the lattice parameter value.

Finally to conclude, the XRD patterns show that the samples are single-phase Wurtzite structure and peaks of no secondary phase are observed. Hence paramagnetism was observed in our system since presence of secondary phases of cobalt will give rise to ferromagnetism (Wang et al. 2006).

The photoluminescence spectra of cobalt-doped ZnO nanopowders (excited at 370 nm using Xe laser source) at room temperature is shown in Fig. 3. The three strong emission peaks ranges from 412 nm to 672 nm is observed. Photoluminescence spectra of $Zn_{1-x}Co_xO$ nanoparticles consist of a Near Band Edge peak of strong ultraviolet emission band centered at 412 nm (3.00 eV), defect level edge peak of blue emission at 471 nm (2.63 eV) and a red emission band at 672 nm (1.84 eV). Ultraviolet emission peak around 412 nm is related to the recombination of free excitons arising from Near band edge transition of ZnO through an exciton–exciton process (Li et al. 2006), while the defect level emission intensity at 471 nm correlates directly with intrinsic defect density. With increasing cobalt concentration, emission intensity of the peak at 412 nm and 471 nm increases exponentially for the concentrations $x = 0.05$ and 0.10, as shown in Fig. 3. Further increasing the concentration, the intensity of the peak decreases due to concentration quenching, which may be correlated to the cluster formation as indicated in the broadening of the XRD (101) peak, for higher doping.

Hence it may be concluded that for room temperature ferromagnetism to occur either free carriers are required (carrier mediated or carrier induced) or formation of oxygen related defect is another essential condition for room temperature ferromagnetism. In this connection that our photoluminescence studies confirm, that no oxygen related defect are found, hence our system exhibit paramagnetism (Pal and Giri 2010). The second DLE peak at 672 nm for red emission contribution is attributed to characteristic transition of the high-spin cobalt levels which gives further support that cobalt ion are substituted for the tetrahedrally coordinated Zn^{2+} ions in the ZnO matrix. Our results were in good agreement with the previous results, which further indicated that cobalt ions were substituted for Zn^{2+} ions in ZnO.

Conclusions

The cobalt-doped ZnO nanopowders were synthesized by citrate sol–gel auto-combustion method. Increasing the cobalt concentration ($x = 0.05$, 0.10 and 0.15) decreases the crystallite size. Solubility of cobalt in ZnO matrix is investigated and increased solubility from 15 to 20 % was found which was attributed to low temperature synthesis. Magnetic measurements reveal paramagnetism among the cobalt ions. Hence no ferromagnetism was observed only paramagnetism was observed due to non availability of free carriers for long range ferromagnetism interaction in our system. When cobalt concentration is increased, peak broadening (101) was observed indicating formation of cobalt cluster (metal–metal) which reduces paramagnetism due to antiferromagnetic interaction and the magnetization values are found to be decreasing. Photoluminescence studies reveal that decrease of intensity of the peak (412 and 471 nm) is due to concentration quenching. Absence of 520 nm peak is related to oxygen vacancy in PL studies also indicates the absence of ferromagnetism in support of our argument.

Acknowledgments The authors are thankful to SAIF, IIT Chennai, for providing Vibrating Sample Magnetometer data, Central instrumentation facility (CIF), Pondicherry University, Puducherry, India for providing Photoluminescence data, Alagappa University, Karaikudi, for providing XRD data.

References

Ando K, Saito H, Jin Z, Fukumura T, Kawasaki M, Matsumoto Y, Koinuma H (2001a) Magneto-optical properties of ZnO-based diluted magnetic semiconductors. J Appl Phys 89:7284

Ando K, Saito H, Jin Z, Fukumura T, Kawasaki M, Matsumoto Y, Koinuma H (2001b) Large magneto-optical effect in an oxide diluted magnetic semiconductor $Zn_{1-x}Co_xO$. Appl Phys Lett 78:2700

Bhat SV, Deepak FL (2005) Tuning the band gap of ZnO by substitution with Mn^{2+}, Co^{2+} and Ni^{2+}. Solid state Commun 135:345

Bouloudenine M, Viart N, Colis S, Dinia A (2004) Bulk $Zn_{1-x}Co_xO$ magnetic semiconductors prepared by hydrothermal technique. Chem Phys Lett 397:73

Coey JMD, Venkatesan M, Fitzgerald CB (2005) Donor impurity band exchange in dilute ferromagneticoxides. Nat Mater 4:173

Dietl T, Ohno H, Matsukura F, Cibert J, Ferrand D (2000) Zener model description of ferromagnetism in zinc-blende magnetic semiconductors. Science 287:1019–1022

Garcia MA, Jimenez-Villacorta F, Quesada A, de la Venta J, Carmona N, Lorite I, Liopis J, Fernandez JF (2010) Surface magnetism in ZnO/Co_3O_4 mixtures. J Appl Phys 107:043906

Hammad TM, Salem JK (2011) Synthesis and characterization of Mg-doped ZnO hollow spheres. J Nanopart Res 13:2205

Hays J, Ponnoose A, Baldner R, Engelhard MH, Peloquin J, Reddy KM (2005) Relationship between the structural and magnetic properties of Co-doped SnO_2 nanoparticles. Phys Rev B 72: 075203

Hays J, Reddy KM, Graces NY, Engelhard MH, Shutthanandan V, Luo M, Xu C, Giles NC, Wang C, Thevuthasan S, Ponnoose A (2007) Effect of Co doping on the structural, optical andmagnetic properties of ZnO nanoparticles. J PhysCondensMatter 19:266203

Jayanthi K, Santha C, Amith GJ, Zahid H, Khanand R, Kotnala K (2010) Fabrication of luminescent, magnetic hollow core nanospheres and nanotubes of Cr-doped ZnO by inclusive coprecipitation method. J Phys Chem C 114:18429–18434

Kobayashi M et al (2005) Characterization of magnetic components in diluted magnetic semiconductor $Zn_{1-x}Co_xO$ by X-ray magnetic circular dichroism. Phys Rev B 72:201201(R)

Lebedeva N, Kuivalainen P (2003) Modeling of ferromagnetic semiconductor devices for spintronics. J Appl Phys 93:9845

Lee HJ, Jeong SY, Cho CR, Park CH (2002) Study of diluted magnetic semiconductor: co-doped ZnO. Appl Phys Lett 81: 4020

Lee S, Kim B-S, Seo S-W, Cho YC, Ki SK, Kim JP, Jeong I-K, Cho C, UkJung C, Koinuma H, Jeong S-Y (2012) A study of the correlation between hydrogen content and magnetism in ZnCoO. J Appl Phys 111:07C304

Li C, Fang G, Fu Q, Su F, Li G, Wu X, Zhao X (2006) Effect of substrate temperature on the growth and photoluminescence properties of vertically aligned ZnO nanostructures. J Crystal Growth 292:19

Ma J, Hao W, Luo R, Xu H (2008) Effect of crystallization quality on ferromagnetism in $Zn_{1-x}Co_xO$ nanopowders. Mat Lett 62:403–406

Pal B, Giri PK (2010) High temperature ferromagnetism and optical properties of Co doped ZnO nanoparticles. J Appl Phys 108: 084322

Quesada A, Garcia MA, Andres M, Hernando A, Fernandez JF, Caballero AC, Martin-Gonzalez MS, Briones F (2006) Ferromagnetism in bulk Co–ZnO. J Appl Phys 100:113909

Rao CNR, Deepak FL (2005) Absence of ferromagnetism in Mn- and Co-doped ZnO. J MaterChem 15:573

Rath C, Mallick P, Pandey D, Sa D, Banerjee A, Mishra NC (2009) Anomalous X-ray diffraction peak broadening and lattice strains in $Zn_{1-x}Co_xO$ dilute magnetic semiconductors. J Phys Condens Matter 21:075801

Risbud AS, Spaldin NA, Chen ZQ, Stemmer S, Ram S (2003) Magnetism in polycrystalline cobalt-substituted zinc oxide. Phys Rev B 68:205202

Sarsari IA, Salamati H, Kameli P, Razavi FS (2011) Optical, structural, and magnetic properties of ZnO: conanoparticles prepared by a thermal treatment of ball milled precursors. J Supercond Nov Magn 24:2293–2298

Segawa Y, Ontomo A, Kawasaki M, Koinuma H, Tang ZK, Yu P, Wong GKL (1997) Growth of ZnO thin film by laser MBE: lasing of exciton at room temperature. Phys status solidi B 202:669

Shannon RD (1976) Revised effective ionic radii and systematic studies of interatomic distances in halides and chalcogenides. Acta Crystallogr A 32:751

Shannon RD, Prewitt CT (1969) Effective ionic radii in oxides and flurides. Acta Crystallogr B 25:925

Shi T, Xiao Z, Xiao ZY, Yin Z, Li X, Wang Y et al (2010) The role of Zn interstitials in cobalt-doped ZnO diluted magnetic semiconductors. Appl Phys Lett 96:211905

Sundaresan A, Bhargavi R, Rangarajan N, Siddesh U, Rao CNR (2006) Ferromagnetism as a universal feature of nanoparticles of the otherwise nonmagnetic oxides. Phys Rev B 74:161306

Ueda K, Hitoshi T, Kawai T (2001) Magnetic and electric properties of transition-metal-doped ZnO films. Appl Phys Lett 79:988

Wang Y, Song Y, Yin S, Yu G, Miao J, Yuan S (2006) Ferromagnetism in manganese and cobalt doped ZnO bulk samples. Mat Sci Eng B 131:9–12

Wang CC, Liu M, Man BY, Chen CS, Jiang SZ, Yang SY, Gao XG, Xu SC, Hu B, Sun ZC, Guo JJ, Hou J (2012) Role of cobalt in room-temperature ferromagnetic Co-doped ZnO thin films. AIP Adv 2:012182

Yang LW, Wu XL, Qiu T, Siu GG, Chau PK (2006) Synthesis and magnetic properties of $Zn_{1-x}Co_xO$ nanorods. J Appl Phys 99:074303

Zener C (1950) Interaction between the d shells in the transition metals. Phys Rev 81:440

Zhang Z, Chen Q, Lee HD, Xue YY, Sun YY (2006a) Absence of ferromagnetism in Co-doped ZnO prepared by thermal diffusion of Co atoms. J Appl Phys 100:043909

Zhang YB, Li S, Tan TT, Park HS (2006b) Optical properties of bulk $Zn_{1-x}Co_xO$ magnetic semiconductors. Solid state commun 137:142